# Van Hove singularities in the paramagnetic phase of the Hubbard model: DMFT study

Rok Žitko,[1] Janez Bonča,[2,1] and Thomas Pruschke[3,4]
[1]*Jožef Stefan Institute, Jamova 39, SI-1000 Ljubljana, Slovenia*
[2]*Faculty of Mathematics and Physics, University of Ljubljana, Jadranska 19, SI-1000 Ljubljana, Slovenia*
[3]*Institute for Theoretical Physics, University of Göttingen, Friedrich-Hund-Platz 1, D-37077 Göttingen, Germany*
[4]*Racah Institute of Physics, The Hebrew University of Jerusalem, Jerusalem, Israel*
(Received 5 August 2009; revised manuscript received 10 November 2009; published 16 December 2009)

Using the dynamical mean-field theory (DMFT) with the numerical renormalization-group impurity solver we study the paramagnetic phase of the Hubbard model with the density of states (DOS) corresponding to the three-dimensional (3D) cubic lattice and the two-dimensional (2D) square lattice, as well as a DOS with inverse square-root singularity. We show that the electron correlations rapidly smooth out the square-root van Hove singularities (kinks) in the spectral function for the 3D lattice and that the Mott metal-insulator transition (MIT) as well as the magnetic-field-induced MIT differ only little from the well-known results for the Bethe lattice. The consequences of the logarithmic singularity in the DOS for the 2D lattice are more dramatic. At half filling, the divergence pinned at the Fermi level is not washed out, only its integrated weight decreases as the interaction is increased. While the Mott transition is still of the usual kind, the magnetic-field-induced MIT falls into a different universality class as there is no field-induced localization of quasiparticles. In the case of a power-law singularity in the DOS at the Fermi level, the power-law singularity persists in the presence of interaction, albeit with a different exponent, and the effective impurity model in the DMFT turns out to be a pseudogap Anderson impurity model with a hybridization function which vanishes at the Fermi level. The system is then a generalized Fermi liquid. At finite doping, regular Fermi-liquid behavior is recovered.

DOI: 10.1103/PhysRevB.80.245112 PACS number(s): 71.27.+a, 71.30.+h, 72.15.Qm

## I. INTRODUCTION

For many materials, it is permissible to consider each electron as moving essentially independently in a static periodic effective potential which takes into account the interactions between the electrons. This point of view received theoretical support through the density-functional theory (DFT) (Ref. 1) and the Kohn-Sham Ansatz,[2] which consists of replacing the full many-body problem with an auxiliary independent-particle problem. DFT calculations are remarkably accurate for wide-band systems, such as simple metals, many semiconductors and insulators, but they are less appropriate for strongly correlated electron systems, such as some transition metals, lanthanides, and their compounds.[3,4]

For noninteracting systems, the density of states (DOS) counts the number of the single-particle levels that may be occupied per unit energy. It can be defined as

$$\rho_0(\omega) = \frac{1}{N}\sum_{\mathbf{k}} \delta(\omega - \epsilon_{\mathbf{k}}), \tag{1}$$

where $\mathbf{k}$ indexes the $N$ single-particle levels with energies $\epsilon_{\mathbf{k}}$. For an infinite system, the sum goes into an integral

$$\rho_0(\omega) = \int \frac{d^d\mathbf{k}}{(2\pi)^d}\delta(\omega - \epsilon_{\mathbf{k}}) = \int \frac{d^{d-1}\mathbf{k}}{(2\pi)^d}\frac{1}{|\nabla \epsilon_k|_{\epsilon_k=\omega}}. \tag{2}$$

Any smooth periodic function has critical points where the gradient vanishes. In a periodic structure such as a crystal, $\epsilon_{\mathbf{k}}$ is periodic in the reciprocal space, therefore $\rho_0(\omega)$ will necessarily have singularities arising from minima, maxima, and saddle points of $\epsilon_{\mathbf{k}}$. For topological reasons, a certain minimum number of these van Hove singularities must be present in any band structure.[5] In two-dimensional (2D) systems, for example, the saddle point in the dispersion gives rise to a logarithmic divergence in the DOS. The van Hove singularities are thought to be particularly important for the physics of low-dimensional systems, for example, in oxide superconductors.[6–10]

For strongly interacting systems, the concept of the single-particle levels is not very useful and one should resort to the techniques from the many-particle theory. In particular, the equivalent of the DOS is the local spectral function

$$\rho(\omega) = -\frac{1}{\pi}\mathrm{Im}[G_{\mathrm{loc}}(\omega + i\delta)], \tag{3}$$

where $G_{\mathrm{loc}}(\omega)$ is the local ($\mathbf{k}$-averaged) Green's function

$$G_{\mathrm{loc}}(\omega) = \frac{1}{N}\sum_{\mathbf{k}} G_{\mathbf{k}}(\omega) \tag{4}$$

with $G_{\mathbf{k}}(z) = \langle\langle c_{\mathbf{k}}; c_{\mathbf{k}}^{\dagger}\rangle\rangle_z$ the momentum-resolved Green's function (electron propagator). In the absence of interactions, $\mathrm{Im}[G_{\mathbf{k}}(\omega + i\delta)] = -\pi\delta(\omega - \epsilon_{\mathbf{k}})$ and Eq. (3) reverts to Eq. (1). The interactions modify the propagation of electrons, thus the spectral function $\rho(\omega)$ differs significantly from the noninteracting DOS $\rho_0(\omega)$ and, in particular, any sharp features such as van Hove singularities are expected to smooth out due to broadening (finite lifetime) effects.

The presence of a diverging DOS at the Fermi level enhances instabilities toward various ordered states, in particular, antiferromagnetism and ferromagnetism,[11] as well as superconductivity.[12] In addition, the underlying paramagnetic metal phase itself is expected to have unusual properties. In this work, we address this regime using the dynamical mean-field theory (DMFT),[13] using the numerical renormalization group (NRG) as the impurity solver.[14–16] We

 

will study the spectral function of the Hubbard model[17–19] in the paramagnetic phase on the three-dimensional (3D) simple cubic lattice (which has square-root singularities at the edges of the band and two further square-root singularities inside the band) and on the two-dimensional square lattice (where a logarithmic singularity is located in the center of the band). We focus on the effects (in particular, on metal-insulator transitions[4]) where local physics plays the key role, thus the use of the DMFT as an approximate method to study finite-dimensional systems is justified. For completeness, we also consider the case of a DOS with an integrable power-law singularity, to wit an inverse square-root DOS. Such divergences can actually arise in real problems, for example, as van Hove singularities in nonbipartite lattices, i.e., they are relevant in connection with DMFT beyond a purely academic interest.

Previous DMFT studies of the Hubbard model generally used either the Bethe lattice or the hypercubic (infinite-dimensional cubic lattice) density of states[13] or, within the local-density approximation plus DMFT approach, a realistic DOS obtained from a density-functional theory calculation for a particular material. Very few works, however, addressed the prototype 2D and 3D simple cubic lattice DOS. The 2D Hubbard model has been studied with the noncrossing approximation,[20] which is limited to finite temperatures on the order of the width of the quasiparticle band. The transition from the 3D to the 2D limit has been studied in the context of the Mott transition in thin layers using the exact diagonalization on small clusters as the impurity solver,[21] incommensurate spin-density waves in doped 2D antiferromagnets have been treated using a generalization of DMFT using an iterative perturbation scheme,[22] and the effects of disorder in the 2D square lattice case have been studied using the Hubbard-I approximation as the impurity solver.[23] So far no work has, however, considered the Hubbard model with 2D and 3D simple cubic lattice DOS using an impurity solver capable of resolving the details in the resulting spectral function, in particular, at low-energy scales.

## II. METHOD

In the limit of infinite dimensions or infinite lattice connectivity, the self-energy in the Hubbard model becomes purely local.[13,24,25] The bulk problem of correlated electrons then maps exactly onto a quantum impurity model with a self-consistently defined noninteracting bath of conduction electrons, in this case an Anderson impurity model.[26–29] To solve the effective impurity model, various nonperturbative techniques can be used, for example, the NRG (Refs. 14, 15, and 30–35) which is particularly suitable to study the low-temperature limit. The NRG calculations in this work were performed for the discretization parameter $\Lambda=2$, with the $z$ averaging over eight values of the twist parameter[36,37] using a modified discretization scheme.[16] Spectral functions were computed using the density-matrix approach[38] and the self-energy trick.[33] The NRG truncation cutoff was set at $E_{\mathrm{cutoff}}=10\omega_N$, where $\omega_N$ is the characteristic energy scale at the $N$th step of the NRG iteration; this is sufficient to obtain results, which are fully converged with respect to the number of states kept. The broadening of spectral functions was performed with a modified log-Gaussian kernel[39] with parameter $\alpha=0.1$. This value is significantly smaller than the broadening parameters traditionally used for DMFT+NRG calculations, thus we are able to achieve relatively good energy resolution even away from the Fermi level.

The input to a NRG calculation step in the DMFT cycle is an effective hybridization function $\Gamma_\sigma(\omega)$ which contains full information about the coupling between the interacting impurity site and the effective noninteracting medium. The output, as required for the DMFT calculation, is the self-energy function $\Sigma_\sigma(\omega)$. The local lattice Green's function is then

$$G_{\mathrm{loc},\sigma}(\omega)=\frac{1}{N}\sum_k G_{k,\sigma}(\omega) \tag{5}$$

$$=\frac{1}{N}\sum_k \frac{1}{[\omega+\mu_\sigma-\Sigma_\sigma(\omega)]-\epsilon_k} \tag{6}$$

$$=\int \frac{\rho_0(\epsilon)d\epsilon}{[\omega+\mu_\sigma-\Sigma_\sigma(\omega)]-\epsilon} \tag{7}$$

$$=G_0[\omega+\mu_\sigma-\Sigma_\sigma(\omega)], \tag{8}$$

where $\rho_0(z)$ is the density of states in the noninteracting model while $G_0(z)$ is the associated free-electron propagator. The local lattice spectral function is then

$$\rho_\sigma(\omega)=-\frac{1}{\pi}\mathrm{Im}[G_{\mathrm{loc},\sigma}(\omega+i\delta)]. \tag{9}$$

The self-consistency condition[13] relates the local lattice Green's function $G_{\mathrm{loc},\sigma}$ and the hybridization function $\Gamma_\sigma$ as

$$\Gamma_\sigma(\omega)=-\mathrm{Im}\{\omega-[G^{-1}_{\mathrm{loc},\sigma}(\omega)+\Sigma_\sigma(\omega)]\}. \tag{10}$$

The DMFT iteration proceeds until two consecutive solutions for the local spectral function differ by no more than some chosen value. To accelerate the convergence to the self-consistency and to stabilize the solutions, we make use of the Broyden mixing.[40]

## III. 3D CUBIC LATTICE DOS

An analytical expression is known for the Green's function for the three-dimensional simple cubic lattice:[41] $G_0^{3\mathrm{D}}(z)=\tilde{G}_0^{3\mathrm{D}}(3z/W)$, where $W$ is the bandwidth and

$$\tilde{G}_0^{3\mathrm{D}}(y)=\frac{1}{y}\frac{\sqrt{1-\frac{3}{4}x_1}}{1-x_1}\left[\frac{2}{\pi}K(k_+^2)\right]\left[\frac{2}{\pi}K(k_-^2)\right],$$

$$k_\pm^2=\frac{1}{2}\pm\frac{1}{4}x_2\sqrt{4-x_2}-\frac{1}{4}(2-x_2)\sqrt{1-x_2},$$

$$x_1=\frac{1}{2}+\frac{1}{6}y^2-\frac{1}{2}\sqrt{1-y^2}\sqrt{1-\frac{1}{9}y^2},$$

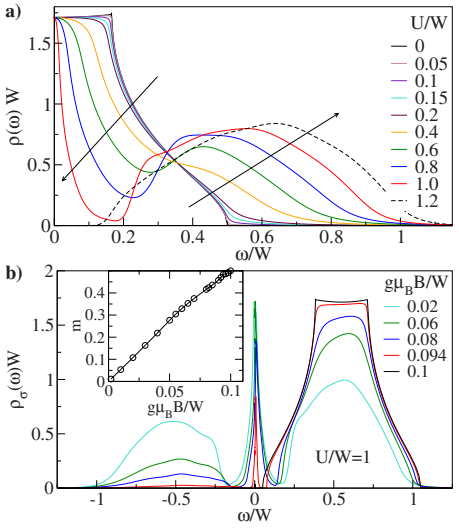


FIG. 1. (Color online) (a) Spectral functions for the Hubbard model with the 3D cubic lattice DOS in the paramagnetic phase at half filling, $T=0$. Due to the particle-hole symmetry only positive frequencies are shown. The arrows indicate the direction of increasing interaction $U$. The dashed curve corresponds to a result for the insulating phase. (b) The evolution of the spectral function as a function of the magnetic field. The inset shows the field dependence of the magnetization.

$$x_2 = \frac{x_1}{x_1 - 1}. \tag{11}$$

Here $K(m)$ is the complete elliptic integral of the first kind, defined as

$$K(m) = \int_0^{\pi/2} \frac{d\theta}{\sqrt{1 - m \sin^2 \theta}} \tag{12}$$

for $m \leq 1$. The behavior of the DOS at the band edges is typical for three-dimensional systems: the DOS goes to zero as $\sqrt{\Delta\omega}$, where $\Delta\omega$ is the distance from the band edge. The DOS is thus continuous, however its derivative diverges. This feature is shared by the DOS of the Bethe lattice with infinite connectivity which is, for this very reason, a common model DOS for three-dimensional systems. Inside the band there are two further square-root singularities where the DOS is continuous but the derivatives are discontinuous and diverging on one side.

All four van Hove singularities smooth out as soon as the interaction is turned on, see Fig. 1(a). At moderate $U/W \sim 0.6$ the spectral function already strongly resembles that obtained for a structureless DOS such as the one for the Bethe lattice with infinite coordination.[34] Nevertheless, the shape of the noninteracting DOS does have an effect on the quantitative details. The Mott-Hubbard metal-insulator (MIT) transition occurs at a value of $U_c/W = 1.165$, which is to be compared with the results for the Bethe lattice, $U_c/W = 1.47$.[34] If the result is rescaled in terms of the effective bandwidth defined through the second moment of the DOS (Ref. 34)

$$W_{\text{eff}} = 4\sqrt{\int_{-W/2}^{W/2} d\epsilon \epsilon^2 \rho(\epsilon)} \approx 0.816W, \tag{13}$$

we obtain $U_c/W_{\text{eff}} = 1.43$, which compares well with the Bethe-lattice result. The feature that $W_{\text{eff}}$ is a rather robust characteristic preferable to the bandwidth has been noted before.[34]

The Hubbard model undergoes a magnetic-field-induced MIT in external magnetic field, the main mechanism on the Bethe lattice being a field-induced quasiparticle mass enhancement (field-induced localization).[13,42,43] The behavior for a 3D cubic lattice DOS is very similar: the quasiparticle peak narrows down and moves slightly away from the Fermi level while the Hubbard bands become increasingly spin polarized and they take the form of the noninteracting DOS, however they do not move much, see Fig. 1(b). The MIT occurs when the quasiparticle peak vanishes. This happens for a field on the scale of the width of the quasiparticle peak in the absence of the field. For $U/W = 1$, for example, the width of the quasiparticle peak at $B=0$ is $0.052W$, while the transition occurs at $g\mu_B B_c = 0.099W$.

## IV. 2D SQUARE-LATTICE DOS

The free-electron propagator on the two-dimensional square lattice is $G_0^{2D}(z) = \tilde{G}_0^{2D}(2z/W)$ with[44]

$$\tilde{G}_0^{2D}(y) = \frac{2}{\pi y} K\left(\frac{1}{y^2}\right), \tag{14}$$

which has a $y \to 0$ expansion

$$\tilde{G}_0^{2D}(y) = \frac{\pi + i(2 \ln y - 4 \ln 2)}{2\pi} + \mathcal{O}(y^2 \ln y), \tag{15}$$

that gives the logarithmic singularity in the density of states at the Fermi level for a half-filled system

$$\rho_0^{2D}(\omega) \sim -\frac{2 \ln(2\omega/W) - 4 \ln 2}{2\pi^2}. \tag{16}$$

The divergence at the Fermi level in the DOS is *not* eliminated as the interaction is turned on, see Fig. 2. The effect of the interaction at low-energy scales is to renormalize the constant part $4 \ln 2/(2\pi^2)$ to smaller values while the logarithmic term keeps the same prefactor. We find that the logarithmic scaling is difficult to achieve numerically to very low energies, where spurious features were observed for energies below $10^{-6}W$. In spite of the diverging spectral function, the Mott metal-insulator transition appears to be of the usual type. With increasing interaction $U$, a region of low spectral density appears before the onset of the logarithmic peak. We find $U_c/W_{\text{eff}} = 1.45$, in agreement with the standard result (it should be noted that for the 2D square lattice DOS we have $W_{\text{eff}} = W$). The value of $U_c$ was determined by studying the sharp resonances in $\text{Im}\,\Sigma(\omega)$ in the metal phase which evolve into the zero-frequency pole in the self-energy for the insulator phase.[29] We extracted their position $X$ as a function of the interaction $U$ and solved for $U_c$ in the equation $X(U_c) = 0$.

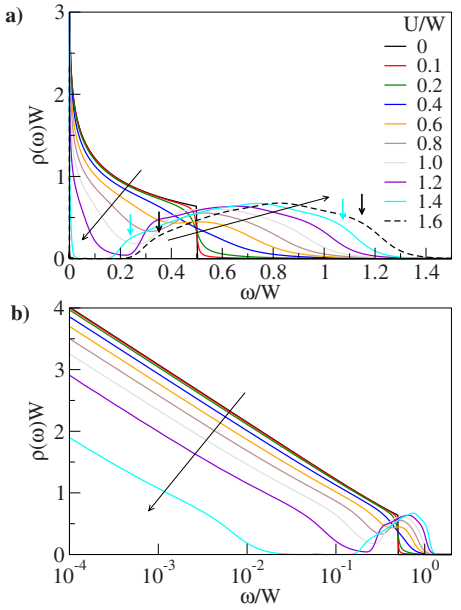


FIG. 2. (Color online) Spectral functions for the Hubbard model with the 2D square-lattice DOS in the paramagnetic phase at half filling, plotted on (a) linear and (b) logarithmic energy scale. The long thin arrows show the direction of increasing $U$. The result plotted with dashed curve is already in the paramagnetic insulator phase. The small thick arrows indicate the weak shoulders in the spectral functions.

For strong interaction, $U \gtrsim W$, the Hubbard bands have a strongly asymmetric shape with pronounced shoulders near the inner band edges, and less pronounced shoulders at the outer band edges, see the features indicated with arrows for $U/W=1.4$ in Fig. 2. These features survive into the insulating phase (indicated with arrows for $U/W=1.6$), which is to be contrasted with the behavior in the case of Bethe and 3D cubic lattice, where the structure at the inner band edge disappears as the transition point is approached.[16,45] The nature of the shoulders observed here is thus different: they reflect the discontinuities at the band edges of the noninteracting DOS.

When the noninteracting system is doped, the logarithmic singularity moves away from the Fermi level. Albeit the energy resolution of NRG is finite at energies away from the Fermi level, it is nevertheless sufficient to study the interaction-induced broadening (the energy resolution of NRG at finite energies has been recently studied in Ref. 16). A plot of the spectral functions as a function of doping is shown in Fig. 3. At finite doping, the imaginary part of the self-energy is finite at the energy of the impurity level, thus the singularity transforms into an asymmetric Lorentzian-type peak. The quasiparticle residue (wave-function renormalization)

$$Z = [1 - \partial\Sigma(\omega)/\partial\omega]^{-1} \tag{17}$$

goes to one with increased doping. It should be noted that at half filling, Re $\Sigma(\omega)$ has a diverging slope, thus $Z \to 0$. The system is thus not a regular Fermi liquid but rather a singular Fermi liquid.[46]

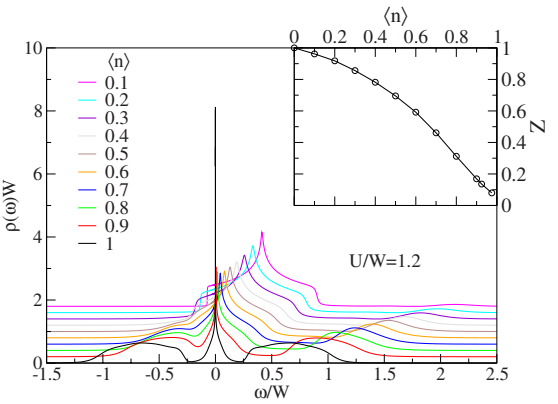


FIG. 3. (Color online) Spectral functions for the Hubbard model with the 2D square-lattice DOS for different doping levels. The curves are offset vertically for clarity. The inset shows the quasiparticle residue as a function of the doping.

The system exhibits unusual properties in the magnetic field. At half filling, the behavior of the quasiparticle peak with increasing field is different from that in the systems with finite DOS at the Fermi level, see Fig. 4. The quasiparticle peak does not narrow down. Instead, as the field increases from zero, the peak shifts away from zero and the singularity is cutoff, but the flanks of the quasiparticle peak are at first affected only very little, see Fig. 4(b). Moreover, for somewhat larger magnetic fields, an additional structure appears above the Fermi energy in the quasiparticle spectrum, see Fig. 4(b), signaling that actually part of the weight removed below the Fermi energy is transferred to the opposite spin channel. As the transition point is approached from

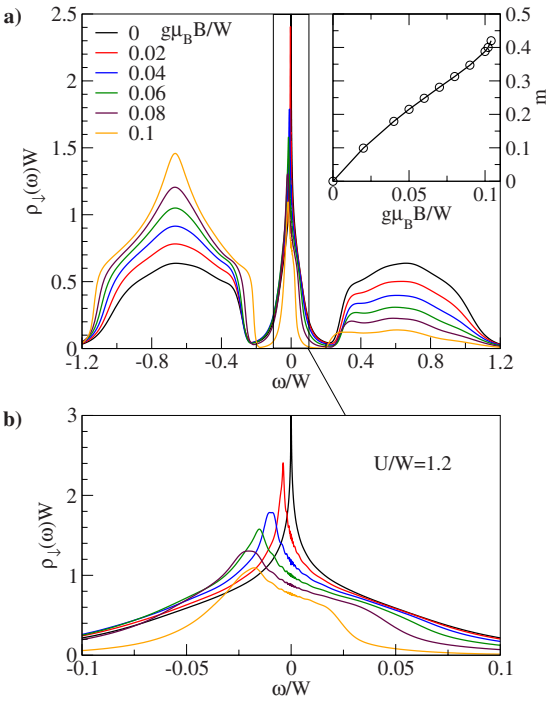


FIG. 4. (Color online) Spectral functions of the Hubbard model with the 2D square-lattice DOS in the magnetic field; half-filling case. The inset shows the field dependence of the magnetization.

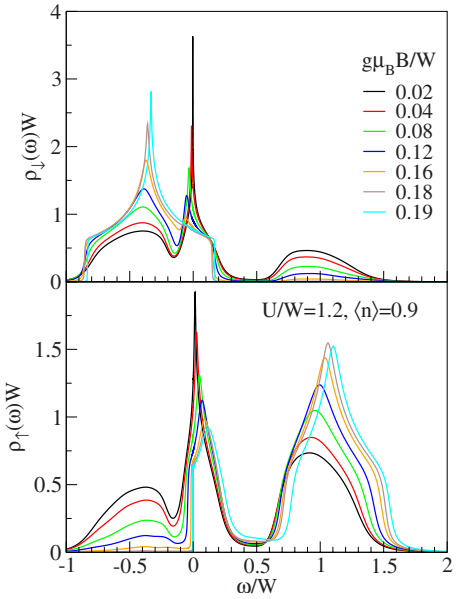


FIG. 5. (Color online) Spectral functions of the Hubbard model with the 2D square-lattice DOS in the magnetic field; finite-doping case.

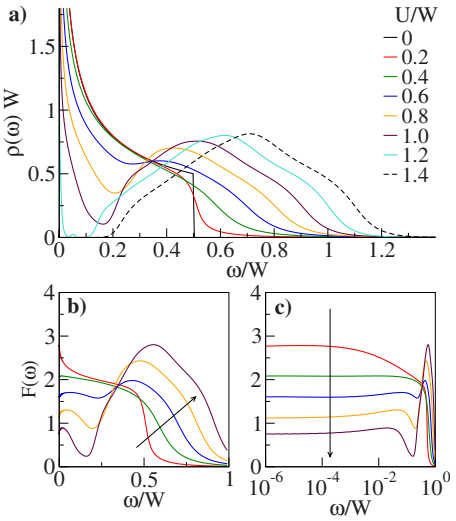


FIG. 6. (Color online) (a) Spectral functions for the Hubbard model with the power-law DOS $|\omega|^{-1/2}$ in the paramagnetic phase at half filling. [(b) and (c)] Rescaled spectral functions on linear and logarithmic energy scale. The arrows show the direction of increasing $U$.

below, we find that the DMFT calculations no longer converge even when the advanced Broyden mixing is used. If one attempts to fix the magnetization instead of the field,[42] it is possible to obtain solutions for somewhat higher magnetizations, although still not all the way to the transition point.

At finite doping, the behavior in the magnetic field becomes more in line with that of systems with nondiverging DOS, see Fig. 5. With increasing field, the quasiparticle peak splits. The majority-spin resonance is reduced in amplitude and eventually disappears as the lower Hubbard band becomes increasingly noninteractinglike. At the same time, the minority-spin resonance becomes wider and transforms into a feature with a sharp edge near the Fermi level. The spin-minority upper Hubbard band is significantly renormalized even for relatively strong magnetic fields. Such behavior is analogous to that found for the Bethe lattice.[47]

## V. DOS WITH POWER-LAW SINGULARITY

Motivated by the unusual features induced by the presence of a logarithmic (i.e., rather mild) singularity at the Fermi level in the DOS of the 2D square lattice, we now study the case of stronger power-law singularities on the example of an inverse square-root DOS,

$$\rho_0(\omega) = \frac{1}{2\sqrt{2}W}|\omega/W|^{-1/2}. \tag{18}$$

The DMFT results presented in Fig. 6(a) indicate that in the presence of the interaction, the power-law singularity remains, however its exponent changes: the spectral functions feature a $\omega^{-\alpha}$ singularity with the exponent around $\alpha \approx 0.40$. The energy below which this power-law scaling of the spectral function holds depends exponentially on the value of $U$ for small $U$, while for $U \gtrsim 0.1W$, it starts to hold essentially on the scale of bare parameters (i.e., $U$ itself).

Interestingly, at half filling the effective quantum impurity model is a pseudogap Anderson model:[48–56] the hybridization function $\Gamma(\omega)$ [see Eq. (10)], shown in Fig. 7(a), has a power-law pseudogap $|\omega|^r$ with exponent $r \approx 0.38$. This is a direct consequence of a diverging spectral function and the imaginary part of the self-energy $\mathrm{Im}\,\Sigma(\omega)$ going to 0 at $\omega = 0$. Our numerical results show that $\mathrm{Im}\,\Sigma(\omega)$ has a cusplike $\omega^\lambda$ singularity with the exponent $\lambda \approx 0.80$, see Fig. 7(b), i.e., the self-energy goes to zero faster than the hybridization function ($r < \lambda$), thus the system can be classified as a generalized Fermi liquid in the sense of Refs. 52 and 53. Within numerical accuracy, the spectral-function exponent $\alpha$ is equal to the hybridization exponent $r$, as expected.[54,55]

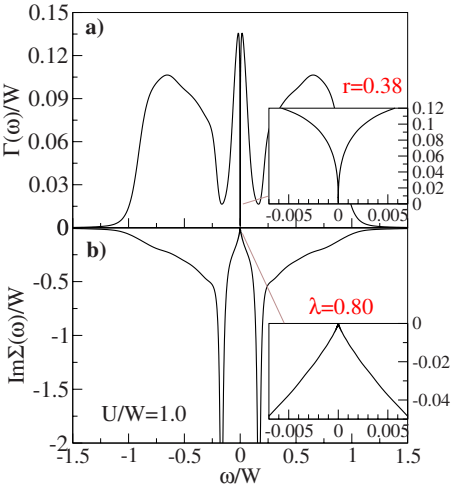


FIG. 7. (Color online) The hybridization function and the imaginary part of the self-energy for the Hubbard model with the power-law DOS $|\omega|^{-1/2}$ in the paramagnetic phase at half filling, $T=0$. The insets are closeups on the low-energy region.

This connection to the pseudogap problem enables us to analyze the low-energy properties in some more detail. As already mentioned above, $\mathrm{Im}\,\Sigma(\omega) \propto |\omega|^{\lambda}$. From the Kramers-Kronig relation between real and imaginary part of $\Sigma(z)$, it follows that[53]

$$\Sigma(\omega) \propto -|\omega|^{\lambda}\{i + \tan[\lambda(\pi/2)]\mathrm{sgn}\ \omega\}. \tag{19}$$

Since the inverse spectral function goes to zero slower (as $|\omega|^{\alpha}$ with $\alpha \approx 0.4$) than both $\omega$ and the self-energy $\Sigma(\omega)$, the self-consistency condition, Eq. (10), reduces at low energies to

$$\Gamma(\omega) = \mathrm{Im}[G_{\mathrm{loc}}^{-1}(\omega)]. \tag{20}$$

Furthermore, taking into account the noninteracting DOS, the local Green's function can be expressed as [Eq. (8)]

$$G_{\mathrm{loc}}(\omega) = G_0[\omega - \Sigma(\omega)], \tag{21}$$

which reduces to $G_{\mathrm{loc}}(\omega) \sim G_0[-\Sigma(\omega)]$ in the limit $\omega \to 0$, since $\Sigma(\omega)$ goes to zero slower than $\omega$. If $G_0(z)$ is the free-electron propagator in a system with power-law DOS $|\omega|^{-R}$, the low-$\omega$ expansion of the hybridization function is found to be

$$\Gamma(\omega) \propto |\omega|^{\lambda R}, \tag{22}$$

which results from combining Eqs. (19)–(21). In our case with $R=1/2$, we have $\lambda \approx 0.8$ and the numerically obtained exponent $r \approx 0.38$ agrees well with the expected value of

$$r = \lambda R = 0.4. \tag{23}$$

The relation $r=\lambda R$ also implies that we have in general $r<\lambda$ for all $R \in [0:1]$ for which the singularity in the density of states is integrable, thus a strong-coupling fixed point (rather than local-moment fixed point) is expected in general and the system will always be a generalized Fermi liquid.

Furthermore, the perturbation theory in $U$ for the pseudogap Anderson impurity model[53] gives a relation $\lambda=2-3r$. Combining this with $r=\lambda R$ we obtain a result for the exponent of the self-energy

$$\lambda = \frac{2}{1+3R}, \tag{24}$$

which is expected to hold in general. For $R=1/2$, this yields $\lambda=4/5$, which is corroborated by our numerical result $\lambda \approx 0.80$.

That the system is a generalized Fermi liquid can be made more explicit by following the suggestion from Ref. 53 and plotting the reduced spectral functions[53]

$$F(\omega) = \pi \sec^2\left(\frac{\pi}{2}\alpha\right)|\omega|^{\alpha}\rho(\omega) \tag{25}$$

in Figs. 6(b) and 6(c). The factor $\pi \sec^2[(\pi/2)\alpha]$ is a convention; it helps to formulate a generalized pinning rule in the pseudogap Anderson impurity model.[53]

The decrease in $F(0)$ with increasing $U$, visible in Figs. 6(b) and 6(c), corresponds to the progressive narrowing of the quasiparticle peak as the MIT is approached. The transition is found to occur for $U_c/W=1.32$ or $U_c/W_{\mathrm{eff}}=1.48$, again in good agreement with the standard result. As for other DOS functions, the Mott MIT proceeds by the same route:[34,57] with increasing $U$ a region of reduced spectral density appears while the weight of the quasiparticle peak decreases until the peak disappears at the critical $U_c$.

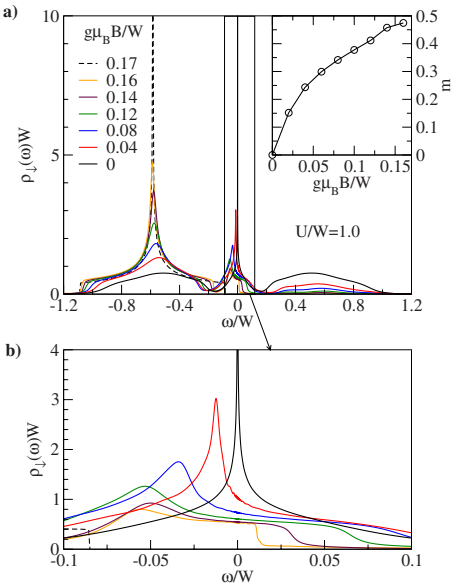


FIG. 8. (Color online) The spectral function of the Hubbard model with the power-law DOS $|\omega|^{-1/2}$ in the magnetic field. The curves are offset vertically for clarity. The inset shows the field dependence of the magnetization.

The behavior in the magnetic field is somewhat similar to that found in the case of logarithmic singularity in DOS, see Fig. 8. With increasing field, the diverging quasiparticle peak transforms into a finite peak shifted away from the Fermi level and its width slightly grows with the field, see the closeup in Fig. 8. At the same time, the majority-spin lower Hubbard band becomes increasingly noninteractinglike with emerging van Hove singularities in its center and sharp band edges. This MIT is thus also not driven by quasiparticle mass enhancement and vanishing width of the quasiparticle band. Note, however, that like for the 2D case we here too observe bad convergence of the DMFT close to the MIT.

Upon doping, the quasiparticle peak transforms smoothly into the van Hove singularity in the center of the empty band, see Fig. 9. At finite doping, the effective hybridization function $\Gamma(\omega)$ no longer attains zero value at $\omega=0$, however it still exhibits a sharp pseudogap feature with a minimum which is shifted away from the Fermi level and where $\Gamma(\omega)>0$. For small doping the minimum still appears cusplike, however it becomes increasingly paraboliclike for larger doping. The evolution of the quasiparticle residue as a function of the doping is shown in the inset to Fig. 9. At half filling, the system is a generalized Fermi liquid, thus $Z=0$. At finite doping, the system is a genuine Fermi liquid with a self-energy which behaves as $\mathrm{Im}\,\Sigma \sim \omega^2$ near the Fermi level.

## VI. CONCLUSION

We have shown that the Hubbard model for the three-dimensional simple cubic lattice has properties very similar

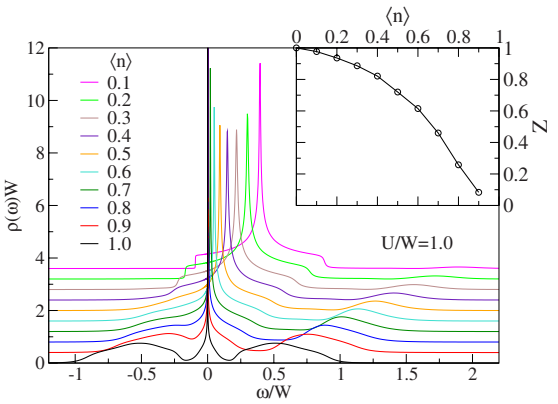


FIG. 9. (Color online) Spectral functions for the Hubbard model with the power-law DOS $|\omega|^{-1/2}$ for different doping levels. The curves are offset vertically for clarity. The inset shows the quasiparticle residue as a function of the doping.

to the Hubbard model on a lattice with a featureless noninteracting density of states (Bethe lattice, hypercubic lattice). More subtle behavior arises in the systems with a density of states which diverges at the Fermi level. These behave as singular Fermi liquids since such singularities are not washed out by the interactions. Their distinguishing characteristic is the different behavior in the magnetic field, in particular, the absence of field-induced quasiparticle localization and a huge sensitivity close to the MIT. This implies a reduced possibility of fully polarizing such systems with external magnetic fields on the order of the width of the quasiparticle band.

This work also demonstrates that the improved discretization scheme for the numerical renormalization group which reduces the discretization artifacts[16] allows to achieve significantly higher spectral resolution at finite energies than in previous DMFT (NRG) studies. This technical improvement thus makes it possible to study the effect of the interactions on spectral features both at very low energies (the traditional forte of the NRG method) and at higher energies, where the required (over)broadening had previously restrained the applicability of the NRG. The improvement results not so much from the $z$ averaging itself, but rather from the modified discretization scheme based on solving the differential equation for the discretization coefficients; this technique is very successful in removing the band edge and other artifacts which would otherwise impair the results.

## ACKNOWLEDGMENTS

This work has been supported by DFG collaborative research center, SFB 602, and Gesellschaft für wissenschaftliche Datenverarbeitung (GWDG). T.P. acknowledges the hospitality of the Racah Institute of Physics. R.Z. and J.B. acknowledge the support of the Slovenian Research Agency (ARRS) under Grants No. Z1-2058 (R.Z.) and No. P1-0044 (J.B.).

[1] P. Hohenberg and W. Kohn, Phys. Rev. **136**, B864 (1964).
[2] W. Kohn and L. J. Sham, Phys. Rev. **140**, A1133 (1965).
[3] G. R. Stewart, Rev. Mod. Phys. **56**, 755 (1984).
[4] M. Imada, A. Fujimori, and Y. Tokura, Rev. Mod. Phys. **70**, 1039 (1998).
[5] L. Van Hove, Phys. Rev. **89**, 1189 (1953).
[6] D. M. Newns, H. R. Krishnamurthy, P. C. Pattnaik, C. C. Tsuei, and C. L. Kane, Phys. Rev. Lett. **69**, 1264 (1992).
[7] K. Gofron, J. C. Campuzano, A. A. Abrikosov, M. Lindroos, A. Bansil, H. Ding, D. Koelling, and B. Dabrowski, Phys. Rev. Lett. **73**, 3302 (1994).
[8] D. H. Lu, M. Schmidt, T. R. Cummins, S. Schuppler, F. Lichtenberg, and J. G. Bednorz, Phys. Rev. Lett. **76**, 4845 (1996).
[9] R. S. Markiewicz, J. Phys. Chem. Solids **58**, 1179 (1997).
[10] V. Y. Irkhin, A. A. Katanin, and M. I. Katsnelson, Phys. Rev. Lett. **89**, 076401 (2002).
[11] R. Hlubina, S. Sorella, and F. Guinea, Phys. Rev. Lett. **78**, 1343 (1997).
[12] J. E. Hirsch and D. J. Scalapino, Phys. Rev. Lett. **56**, 2732 (1986).
[13] A. Georges, G. Kotliar, W. Krauth, and M. J. Rozenberg, Rev. Mod. Phys. **68**, 13 (1996).
[14] K. G. Wilson, Rev. Mod. Phys. **47**, 773 (1975).
[15] R. Bulla, T. Costi, and T. Pruschke, Rev. Mod. Phys. **80**, 395 (2008).
[16] R. Žitko and T. Pruschke, Phys. Rev. B **79**, 085106 (2009).
[17] J. Hubbard, Proc. R. Soc. London, Ser. A **276**, 238 (1963).
[18] J. Kanamori, Prog. Theor. Phys. **30**, 275 (1963).
[19] M. C. Gutzwiller, Phys. Rev. Lett. **10**, 159 (1963).
[20] T. Pruschke, T. Obermeier, J. Keller, and M. Jarrell, Physica B: Condensed Matter **223-224**, 611 (1996).
[21] M. Potthoff and W. Nolting, Eur. Phys. J. B **8**, 555 (1999).
[22] M. Fleck, A. I. Liechtenstein, A. M. Oleś, L. Hedin, and V. I. Anisimov, Phys. Rev. Lett. **80**, 2393 (1998).
[23] Y. Song, R. Wortis, and W. A. Atkinson, Phys. Rev. B **77**, 054202 (2008).
[24] W. Metzner and D. Vollhardt, Phys. Rev. Lett. **62**, 324 (1989).
[25] E. Müller-Hartmann, Z. Phys. B: Condens. Matter **74**, 507 (1989).
[26] A. Georges and G. Kotliar, Phys. Rev. B **45**, 6479 (1992).
[27] M. J. Rozenberg, X. Y. Zhang, and G. Kotliar, Phys. Rev. Lett. **69**, 1236 (1992).
[28] M. Jarrell, Phys. Rev. Lett. **69**, 168 (1992).
[29] X. Y. Zhang, M. J. Rozenberg, and G. Kotliar, Phys. Rev. Lett. **70**, 1666 (1993).
[30] H. R. Krishna-murthy, J. W. Wilkins, and K. G. Wilson, Phys. Rev. B **21**, 1003 (1980).
[31] O. Sakai, Y. Shimizu, and T. Kasuya, J. Phys. Soc. Jpn. **58**, 3666 (1989).
[32] T. A. Costi, A. C. Hewson, and V. Zlatic, J. Phys.: Condens. Matter **6**, 2519 (1994).
[33] R. Bulla, A. C. Hewson, and T. Pruschke, J. Phys.: Condens. Matter **10**, 8365 (1998).
[34] R. Bulla, Phys. Rev. Lett. **83**, 136 (1999).

[35] T. Pruschke, R. Bulla, and M. Jarrell, Phys. Rev. B **61**, 12799 (2000).
[36] H. O. Frota and L. N. Oliveira, Phys. Rev. B **33**, 7871 (1986).
[37] V. L. Campo and L. N. Oliveira, Phys. Rev. B **72**, 104432 (2005).
[38] W. Hofstetter, Phys. Rev. Lett. **85**, 1508 (2000).
[39] A. Weichselbaum and J. von Delft, Phys. Rev. Lett. **99**, 076402 (2007).
[40] R. Žitko, Phys. Rev. B **80**, 125125 (2009).
[41] G. S. Joyce, J. Phys. A **5**, L65 (1972).
[42] L. Laloux, A. Georges, and W. Krauth, Phys. Rev. B **50**, 3092 (1994).
[43] J. Bauer, Eur. Phys. J. B **68**, 201 (2009).
[44] E. N. Economou, *Green's Functions in Quantum Physics* (Springer, Berlin, 2006).
[45] M. Karski, C. Raas, and G. S. Uhrig, Phys. Rev. B **72**, 113110 (2005).
[46] C. M. Varma, Z. Nussinov, and W. van Saarloos, Phys. Rep. **361**, 267 (2002).
[47] J. Bauer and A. C. Hewson, Phys. Rev. B **76**, 035118 (2007).
[48] D. Withoff and E. Fradkin, Phys. Rev. Lett. **64**, 1835 (1990).
[49] K. Chen and C. Jayaprakash, Phys. Rev. B **52**, 14436 (1995).
[50] K. Ingersent, Phys. Rev. B **54**, 11936 (1996).
[51] R. Bulla, T. Pruschke, and A. C. Hewson, J. Phys.: Condens. Matter **9**, 10463 (1997).
[52] C. Gonzalez-Buxton and K. Ingersent, Phys. Rev. B **57**, 14254 (1998).
[53] M. T. Glossop and D. E. Logan, Eur. Phys. J. B **13**, 513 (2000).
[54] R. Bulla, M. T. Glossop, D. E. Logan, and T. Pruschke, J. Phys.: Condens. Matter **12**, 4899 (2000).
[55] D. E. Logan and M. T. Glossop, J. Phys.: Condens. Matter **12**, 985 (2000).
[56] M. Vojta and R. Bulla, Eur. Phys. J. B **28**, 283 (2002).
[57] G. Moeller, Q. Si, G. Kotliar, M. Rozenberg, and D. S. Fisher, Phys. Rev. Lett. **74**, 2082 (1995).